International Journal of Machine Tools & Manufacture 89 (2015) 86–94

Contents lists available at ScienceDirect

International Journal of Machine Tools & Manufacture

journal homepage: www.elsevier.com/locate/ijmactool

Geometric prediction of conic tool in micro-EDM milling with fix-length compensation using simulation

Lenan Zhang, Jianyi Du, Xiaoshun Zhuang, Zhiliang Wang, Jingyu Pei *

School of Mechanical Engineering, Shanghai Jiao Tong University, 800 Dongchuan Road, Shanghai, PR China

ARTICLE INFO

Article history:
Received 25 May 2014
Received in revised form
3 September 2014
Accepted 15 November 2014
Available online 20 November 2014

Keywords:
Micro EDM milling
Fix-length compensation
Geometric simulation
Cone shaped tool

ABSTRACT

Micro-EDM milling is an effective machining process for three-dimensional micro-cavity of high hardness materials. However, tools wear sharply in micro-milling, thus several compensation methods are applied. The present study examines the fix-length compensation method, and the initial experiments show that a cone-shaped tool end is formed with this compensation method. Because the cone angle is of great importance in the determination of the fix-length compensation parameters in the machining procedure, a clear explanation of the forming mechanism and precise prediction are of great necessity. First, the tool and the workpiece were geometrically and mathematically modeled as two-dimensional matrices. Second, the machining process was divided into three parts including sparking, horizontal feeding and vertical feeding. Finally, a series of experiments were conducted in order to verify the accuracy of the simulation. The results show that the relative error of the simulation compared to the experimental data is within 4% under most machining conditions. The developed model can thus be used to predict the machined surface of the tool and the workpiece and can also provide a better understanding for the mechanism of the cone shaped tool end.

1. Introduction

Micro-manufacturing requires higher machining stability and precision, which focuses on both dimensional accuracy and surface properties. As a micro-manufacturing method, micro-electric discharge machining (micro-EDM) [1] has been widely applied for its uniqueness in material removal mechanism. First, for a non-contact machining method with no macro-mechanical force during the process, EDM can process electric conductive materials regardless of the hardness. Second, since the diameter of the micro-hole machined by micro-EDM can be as small as 5 μm [2], EDM has really high precision. Third, EDM is capable of milling complex three-dimensional cavities.

In micro-EDM milling, cylinder-shaped micro-electrodes are applied to process three-dimensional cavities. The machining follows a movement control program similar to the conventional milling [3], mainly affected by several parameters including the open circuit voltage, peak gap current, spark-on time, sparking gap, the tool wear ratio, etc.

As the tool wear accounts for one of the main factors affecting the machining precision in micro-EDM milling, in the literature a number of studies have been carried out focusing on the compensation of electrode during the machining process for precision improvement. Yu et al. [4] proposed the uniform wear method (UWM). Based on the layer-by-layer machining process, the thickness of each layer is set small enough for the recovery of the electrode tip, resulting in the maintenance of the electrode shape during the machine. Kuo et al. [5] introduced a technology called linear compensation which continuously compensated for the tool wear along the tool path. The surface precision was improved. However, the method was not suitable for complicating three-dimensional shape milling. Bleys et al. [6] presented a compensation method based on real-time tool wear sensing which could deal with unexpected shape. The downward motion was controlled according to the tool wear ratio calibrated in advance, thus the error caused by longitudinal tool wear was eliminated. Pei et al. [7] proposed the fix-length compensation method while a revolving electrode fed a fix-length between two compensation operations. The fix-length depends on the compensation accuracy and the layer thickness. As the method was able to suppress the influence of tool wear on the surface precision, both the dimensional accuracy and the shape accuracy were optimized.

* Corresponding author. Fax: +86 021 62932611.
E-mail addresses: zhanglenan@sjtu.edu.cn (L. Zhang), dujianyivapor@sjtu.edu.cn (J. Du), zhuangxs@sjtu.edu.cn (X. Zhuang), darren0509@sjtu.edu.cn (Z. Wang), jypei@sjtu.edu.cn (J. Pei).

http://dx.doi.org/10.1016/j.ijmachtools.2014.11.007
0890-6955/

The development of simulation technology has contributed to a better understanding of EDM process. The geometry simulation, in particular, has been widely applied to illustrate the shape variation of both the electrode and the workpiece during machining. Kunieda and Kiyohara [8] developed a geometric simulation for EDM die-sinking process to achieve the proper tool electrode shape. Several coupling influential factors were taken into account including the tool wear, debris particle concentration and the tool motion. Yu et al. [9] introduced a geometric simulation based on the uniform tool wear assumption, a model valid for tool wear prediction and suitable for both macro- and micro-EDM slot process. Zhao et al. [10] proposed a geometrical model for linear motor driven EDM die-sinking process using the Z-map method, in which craters were assumed to be concave shaped and the EDM process was described more precisely compared with the cube shaped one. Young et al. [11] developed a two-dimensional geometric simulation model of EDM drilling with a cylindrical tool, which took both end and corner wear of tool into consideration. The model was suitable for the online compensation method. Segon Heo et al. [12] introduced a three-dimensional geometric simulation method for micro-EDM milling process to predict the machined geometry. The model could be used to optimize parameters of actual machining process and provide improvements for CNC programs to implement the compensation.

What is missing in the published studies is simulation with the fix-length compensation method, without which it is impossible to explain the forming of cone shaped electrode and to predict the cone angle. The present study, an attempt to fill the gap, aims to predict the cone angle which has significant effect on the machining precision of 3D micro-cavity. For this, a two-dimensional geometric simulation model is developed for micro-EDM milling process based on the fix-length compensation method. And the machining process is divided into three stages, sparking, feeding, and fix-length compensation. A series of experiments are conducted to verify the effectiveness of the model and simulation.

2. Process of the fix-length compensation

During the EDM milling process, the electrode is processed on the surface of the workpiece by a specific path $g(x)$, but the real processing surface is described by a different trajectory $H(x)$ as illustrated in Fig. 1, because wear on the electrode is inevitable during the process [9]. The fix-length compensation method is therefore adopted to minimize the impact of electrode wear on the accuracy of the workpiece.

As is shown in Fig. 2, the fix-length compensation method consists of three steps. First, the electrode starts processing at the initial position A. Second, it reaches B with horizontal feed L_{comp}. Third, the electrode gets to C with a vertical feed l_{comp}. In this method, H_{comp}, layer thickness, stands for the target depth for one layer of ED-milling, and L_{comp} is the compensation length for the electrode to move horizontally before one vertical feed is triggered. l_{comp}, the compensation accuracy, is a preset value. As H_{comp} and L_{comp} are small enough in the real process, which range between 10 μm and 100 μm, while compensation accuracy is usually within 1 μm, this method can process surface with high accuracy.

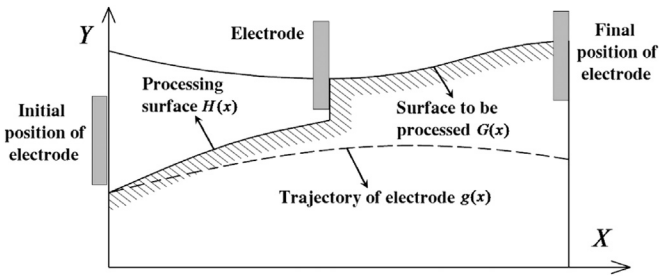

Fig. 1. Machined bottom profile by EDM milling [9].

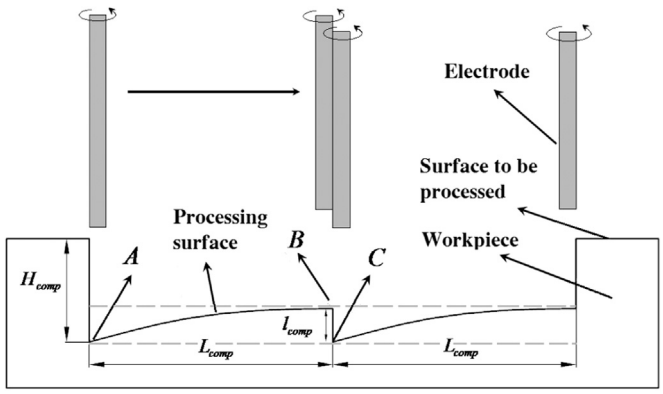

Fig. 2. Theory of fix-length compensation in EDM milling [7].

3. Modeling of EDM fix-length compensation milling

In the milling process, the tool is cylindrical and it has three kinds of motions during the process – rotation around a spindle, milling feed along the horizontal direction and compensation in the vertical direction, as shown in Fig. 3. Because the end face of the electrode will become cone-shaped and stabilize after moving for a certain distance, the electrode is nearly axially symmetrical during the whole machining process. Thus to simplify the modeling, the simulation is depicted in two dimensions. In this way, the axial section of the tool and the longitudinal section of the

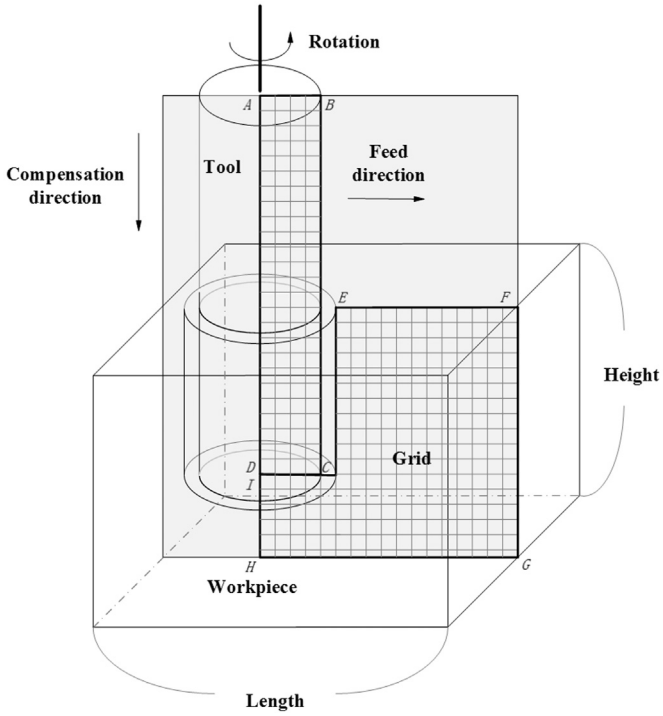

Fig. 3. Simplification of EDM machining process to a pre-drilled and two-dimensional model.

workpiece can represent machining conditions and show the final shapes of both the electrode and the workpiece. As demonstrated in Fig. 3, the tool is modeled in rectangle *ABCD*, and the workpiece is simplified as polygon *EFGHIJ*.

There are six assumptions in the simulation.

1. The cylindrical electrode remains axially symmetrical during the whole machining process due to rotation.
2. There is only one spark in each simulation step [10].
3. The spark is generated on such a position where the gap between two points on the electrode and the workpiece is the shortest. Other factors of the sparking are ignored, such as corona discharging [13].
4. The energy delivered by one spark in each simulation step is a constant. That is to say, the removed volume of the material on the electrode is a constant [6,14].
5. The size of plasma channel is ignored. In other words, the energy delivered by one spark is transferred point to point, rather area to area 15.
6. The crater generated by one spark is hemispheric. All the material in the hemisphere is removed by the dielectric fluid.

This model has three main parts, namely sparking, horizontal feeding and vertical feeding process, which are all based on the geometrical modeling of the electrode and the workpiece. Flowchart in Fig. 4 illustrates these parts and the procedure of the whole simulation.

3.1. Modeling of electrode and workpiece geometries

The cross-sections of the electrode and the workpiece are depicted in two dimensions. The cylindrical electrode is assumed to be axially symmetrical, and the cross-section through the axial line can represent the shape of the electrode in the whole manufacturing process. At the beginning of the simulation, the initial drilling process is considered finished and the depth of the drilling hole is the layer thickness, therefore the workpiece takes the shape of polygon (*EFGHIJ*), as shown in Fig. 3.

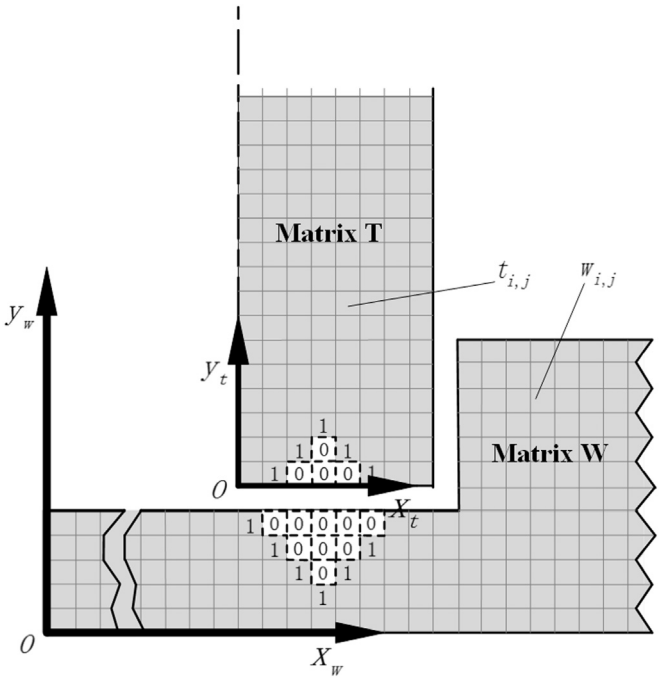

Fig. 5. The establishment of relative and absolute coordinates.

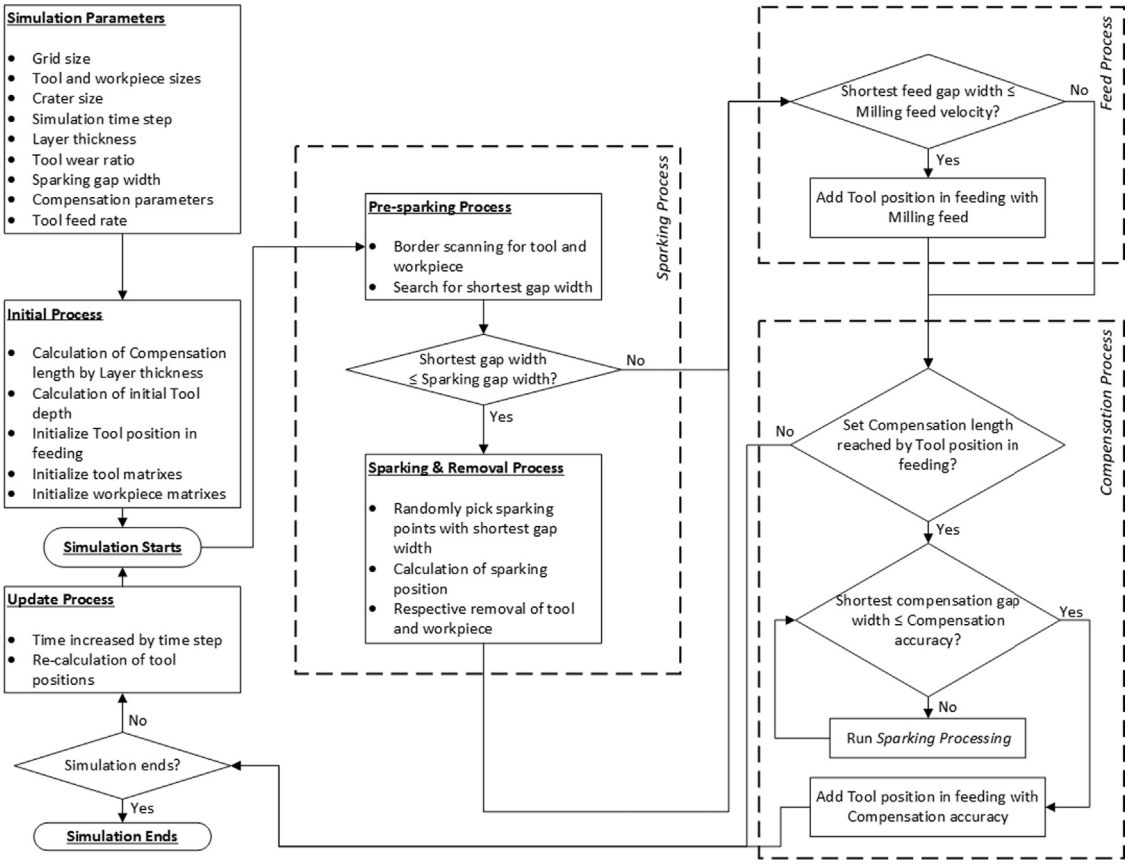

Fig. 4. Flowchart of the developed fix-length compensation method simulation model.

Then grids are applied to partition the electrode and the workpiece into an enormous number of tiny square elements with the same size shown in Fig. 3. In fact, such grids can be described as two-dimensional matrices, namely **T** and **W** in Fig. 5. Each matrix element has only two possible values, 1 for Not Removed and 0 for Removed.

In this model, the electrode is moving in both horizontal and vertical directions, while the workpiece is considered to be fixed. Therefore, an absolute coordinate X_wOY_w is set on the workpiece, and a relative coordinate X_tOY_t on the electrode, as illustrated in Fig. 5. In the relative coordinates, the position of elements of the tool can be described as the following:

$$\begin{aligned} x^t_{t,i} &= l_{grid} \times (i-1) + x^t_{t,1} i \\ &= 1, 2, 3, \ldots n_{t,x}, \quad n_{t,x} \\ &= \left[\frac{R_t}{l_{grid}}\right] + 1 y^t_{t,j} \\ &= l_{grid} \times (j-1) + y^t_{t,1} j \\ &= 1, 2, 3, \ldots n_{t,y}, \quad n_{t,y} \\ &= \left[\frac{L_t}{l_{grid}}\right] + 1 \end{aligned} \tag{1}$$

where $(x^t_{t,i}, y^t_{t,j})$, $(x^t_{t,1}, y^t_{t,1})$, l_{grid}, R_t, and L_t are the position of the element $t_{i,j}$ in the relative coordinate, the position of the element $t_{1,1}$ in the relative coordinate, the side length of the element square, the radius of tool and the length of tool respectively.

While in absolute coordinates, elements of the workpiece can be described as the following:

$$\begin{aligned} x^w_{w,i} &= l_{grid} \times (i-1) + x^w_{w,1} i \\ &= 1, 2, 3, \ldots n_{w,x}, \quad n_{w,x} \\ &= \left[\frac{L_w}{l_{grid}}\right] + 1 y^w_{w,j} \\ &= l_{grid} \times (j-1) + y^w_{w,1} j \\ &= 1, 2, 3, \ldots n_{w,y}, \quad n_{w,y} \\ &= \left[\frac{H_w}{l_{grid}}\right] + 1 \end{aligned} \tag{2}$$

where $(x^w_{w,i}, y^w_{w,j})$, $(x^w_{w,1}, y^w_{w,1})$, L_w, and H_w are the position of the element $w_{i,j}$ in the absolute coordinate, the position of $w_{1,1}$, the length of the workpiece and the height of the workpiece respectively.

With simple coordinate transformation, element of tool in absolute coordinates is shown as

$$\begin{aligned} x^w_{t,i} &= x_{t,init} + x^t_{t,i} + \int V_{feed} dt, \quad i \\ &= 1, 2, 3, \ldots n_{t,x} y^w_{t,j} \\ &= y_{t,init} + y^t_{t,j} + \int V_{comp} dt, \quad j \\ &= 1, 2, 3, \ldots n_{t,y} \end{aligned} \tag{3}$$

where $(x^w_{t,i}, y^w_{t,j})$, $(x_{t,init}, y_{t,init})$, and $(x^t_{t,i}, y^t_{t,j})$ are the position of the element $t_{i,j}$ in the absolute coordinate, the initial position of the element $t_{1,1}$ in the absolute coordinate and the position of the element $t_{i,j}$ in the relative coordinate, respectively. And the V_{feed} and V_{comp} are the feed rate in the horizontal direction and the compensation velocity in the vertical direction, which satisfy the following equations:

$$V_{feed} = \begin{cases} C_1 & \text{feedprocess} \\ 0 & \text{otherwise} \end{cases} V_{comp} = \begin{cases} C_2 & \text{compensationprocess} \\ 0 & \text{otherwise} \end{cases} \tag{4}$$

Besides defining the grids and their positions, as shown in Figs. 4 and 5, the model also involves some machining information: the sizes of the electrode and the workpiece to determine the ones in matrices; the layer thickness and the gap between the electrode and the workpiece to calculate the origin of relative coordinates in absolute ones; milling feed rate to get the horizontal feed velocity of the electrode matrix; compensation accuracy to set the vertical compensation velocity in fix-length compensation.

3.2. Modeling of sparking process

There are two main steps in the sparking process. First, all point pairs with the shortest distance are sought out on the surface of the electrode and the workpiece. If that distance is within the sparking gap, sparking is generated between one randomly chosen point pair, defined as the sparking point pair. Then a certain volume of materials are removed from the electrode and the workpiece. Otherwise, sparking is skipped for this time step, which is the unit time in simulation determined by the maximum spark frequency.

According to assumption (2), there is only one single spark generated in one simulation step. So the time step is shown as

$$\Delta t = \frac{1}{f_{spark}} \tag{5}$$

where Δt is the unit time in each simulation step and f_{spark} is the maximum sparking frequency.

3.2.1. Searching for the sparking points

According to assumption (3), the only factor that affects sparking occurrence is the gap between the electrode and the workpiece. In this model, sparking only occurs when the shortest distance between the electrode and the workpiece face is less than the sparking gap, which is determined by the material of dielectric and open circuit voltage [13]. As the dielectric fluid and the voltage in the experiment are set as kerosene-based mixture and 200 V A respectively, the sparking gap is a constant of 9 μm in the simulation.

Fig. 6 shows the location of the sparking points, where area is the search area to find the shortest distance. As the length of d_2 is

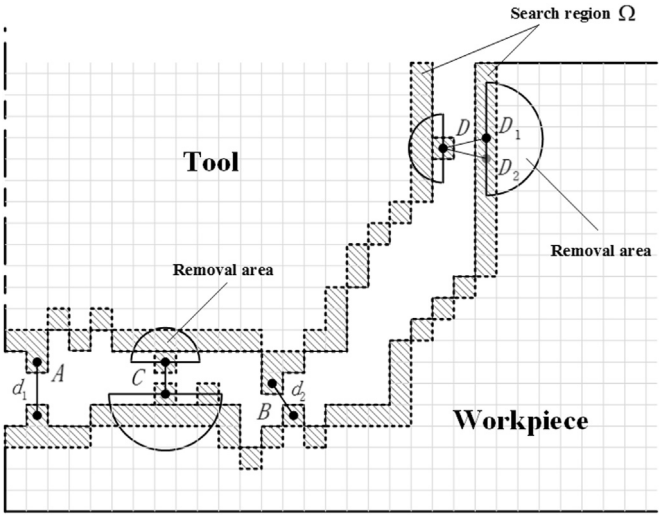

Fig. 6. Schematic diagram of sparking process.

shorter than d_1, the points pair B is chosen. Point D_1 and D_2 are randomly picked as the sparking point, as $DD_1 = DD_2$.

The distance between any arbitrary two points on the electrode and the workpiece is calculated by the following equation:

$$d = \sqrt{(x_{t,i}^w - x_{w,m}^w)^2 + (y_{t,y}^w - y_{w,n}^w)^2} \tag{6}$$

where d is the distance between two elements on the surface of tool and workpiece. (x_t, y_t) is the absolute coordinate for an element in the search region of the electrode, while (x_w, y_w) is the absolute coordinate for an element in the search region of the workpiece.

Sparking is generated when the following condition is satisfied, where D_{spark} is the sparking gap:

$$d \le D_{spark} \tag{7}$$

3.2.2. Modeling of material removal

According to assumption (4), the crater sizes of the electrode and the workpiece are fixed, for spark-on time, gap current and voltage are constant and a fixed amount of energy acts on both the electrode and the workpiece in every spark [6,15]. Moreover, the materials of the electrode and the workpiece remain unchanged, and there is hence a stable tool wear ratio for every step. To simplify the following processes, crater can, according to assumptions (5) and (6), be described as a semicircle, whose radius can be gauged in experiments.

After the sparking point pair is chosen, a circle is then drawn on the workpiece with its origin at this point and the preset radius. All materials in such a circular area are removed. Accordingly, the corresponding values of the workpiece matrix are turned from 1 to 0. Meanwhile, for the tool removal, similar rules are applied to the electrode but with a different radius of crater, which can be calculated with tool wear ratio by the following formula [9]:

$$r_t = r_w \theta^{1/3} \tag{8}$$

where r_t and r_w are the radius of the crater on tool and workpiece respectively and θ is the tool wear ratio.

Fig. 6 demonstrates the removal process, where a certain volume of material surrounding point pair C and D are removed.

At the end of the removal process, boundaries of the electrode and the workpiece are updated.

In the feeding process simulation, both peripheral feed and face feed are taken into consideration [12].

3.3. Modeling of the feeding process

The sparking process as discussed in Section 3.2 is repeated till the gap grows wider and exceeds the breakdown voltage gap. Then, as sparking halts, the feeding process starts. With the horizontal movement of the electrode towards the workpiece, the gap decreases step by step and finally meets the sparking gap condition, at which point sparking restarts.

The feed is determined by the feed rate of machine as the following:

$$\Delta S_{feed} = V_{feed} \Delta t \tag{9}$$

where ΔS_{feed} is the distance of feed in one simulation step, V_{feed} is the feed rate in the horizontal direction, Δt is the unit time in each simulation step.

When the feeding process starts, coordinates of the electrode's elements are transformed as the following:

$$\begin{aligned} x_{t,i}^w &= x_{t,i}^w + \Delta S_{feed}, \quad i \\ &= 1, 2, 3, \ldots n_{t,x} y_{t,i}^w \\ &= y_{t,i}^w, \quad j \\ &= 1, 2, 3, \ldots n_{t,y} \end{aligned} \tag{10}$$

After each feeding process, positions of the electrode's elements are updated and are used in the sparking process of next round.

3.4. Modeling of the vertical feeding process

During the horizontal feeding process as discussed in the above section, the electrode is being worn, thus the vertical feed is necessary in order to maintain the layer thickness. The periodical vertical feed is the characteristic feature of the fix-length compensation process.

Both length of compensation and compensation accuracy are considered in the simulation.

It is rather important to note that the fix-length compensation is of high priority [7]. That is to say, when the distance of the electrode's horizontal movement is equal to or bigger than the preset compensation length L_{comp}, the vertical feed with distance set by compensation accuracy l_{comp} is triggered. If the electrode is blocked vertically by the workpiece, sparking will start with no horizontal feeding until there is enough space for vertical feeding.

According to the theory of fix-length compensation [7], compensation accuracy is set by accuracy of machine itself, the layer thickness is set before machining, and the compensation length can be calculated.

In initialization process, the length of compensation will be determined firstly. After that, compensation availability will be judged in every simulation step. If horizontal position is multiple of compensation length, compensation process starts as described above. It is emphasized that once condition for fixed compensation length meets, such compensation for vertical feed will be of the highest priority, during which sparking and removal processes are both available for accomplishment. After this compensation process, matrix of tool will be transformed to

$$x_{t,i}^w = x_{t,i}^w, \quad i = 1, 2, 3 \ldots n_{t,x} y_{t,i}^w = y_{t,i}^w - l_{comp}, \quad i = 1, 2, 3 \ldots n_{t,y} \tag{11}$$

Positions of electrode will be refreshed and stored for next simulation step.

For now, one simulation step is completed. Such steps will repeat again and again, including the same sparking, feed and compensation processes as stated above.

Table 1
Simulation parameters.

Item	Unit	Value
Grid size (l_{grid})	μm	0.5
Tool diameter ($2R_t$)	μm	200
Crater diameter on workpiece (r_w)	μm	3
Length of workpiece (L_w)	μm	5000
Height of workpiece (H_w)	μm	400
Simulation time step (Δt)	μs	100
Layer thickness (H_{comp})	μm	43.5
Tool wear ratio (θ)	\	11.9%
Sparking gap width (D_{spark})	μm	9
Length of compensation (L_{comp})	μm	60
Compensation accuracy (l_{comp})	μm	1
Tool feed rate (V_{feed})	μm/s	60

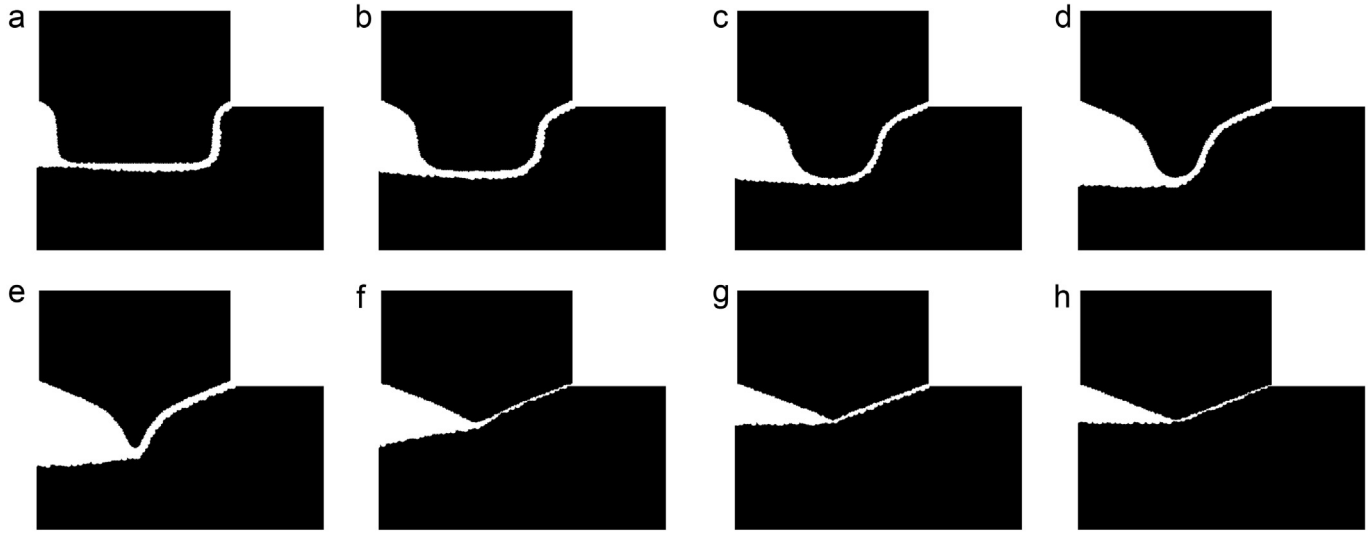

Fig. 7. The forming process of cone shaped electrode using simulation: (a) milling 200 μm, (b) milling 450 μm, (c) milling 700 μm, (d) milling 900 μm, (e) milling 1100 μm, (f) milling 1400 μm, (g) milling 1800 μm and (h) milling 2300 μm.

4. The forming of cone-shaped electrode using simulation

To demonstrate the formation of cone shaped electrode, a simulation is conducted. The simulation parameters are shown in Table 1 and these parameters are in accordance with real machining parameters in Table 3.

The simulation results are depicted in Fig. 7. According to the results, the forming process can be divided into three stages, namely starting stage, cone shaping stage and steady stage.

The starting stage is shown in Fig. 7(a) or region AB in Fig. 8. After the drilling process, the electrode starts the milling process. With parameters of fix-length compensation mentioned above, the milling length at the starting stage is about 400 μm. At this stage, peripheral milling plays the key role in shaping the electrode with the following characteristics:

1. Diameter of the end face the in milling process decreases sharply.
2. The profile of the electrode is shaped as an *S* curve symmetrical with the vertical axis, and no clear cone face is shaped.

The cone shaping stage is shown in Fig. 7(b)–(f) or region BC in Fig. 8. With parameters of fix-length compensation mentioned above, the milling length for this stage is approximately 1100 μm. At this stage during the compensation process, when the vertical feed is hampered, the removal of the face milling is activated and added to that of peripheral milling. Both of them contribute to the conic shape. In the end, the profile of the electrode surface is shaped as two tilting lines symmetrical with the vertical axis, shown in Fig. 7(f).

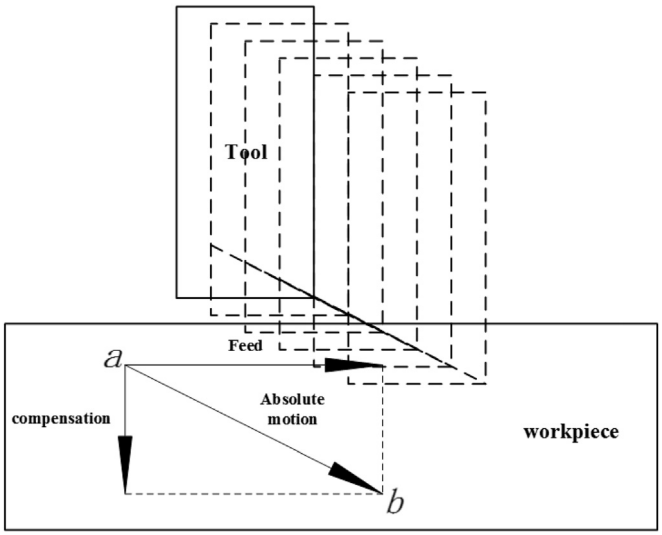

Fig. 9. Relative motion of electrode to workpiece.

The cone shaping stage features the following characteristics:

1. The end face for the electrode remains flat, and periphery of the electrode is shaped as a symmetrical *S*.
2. As the process continues, the area of the flat end face decreases, while the *S* curve flattens from the top to the bottom gradually.
3. As a result of (2), the depth of the electrode involved in sparking keeps changing, thus making the depth of the cavity unsteady.

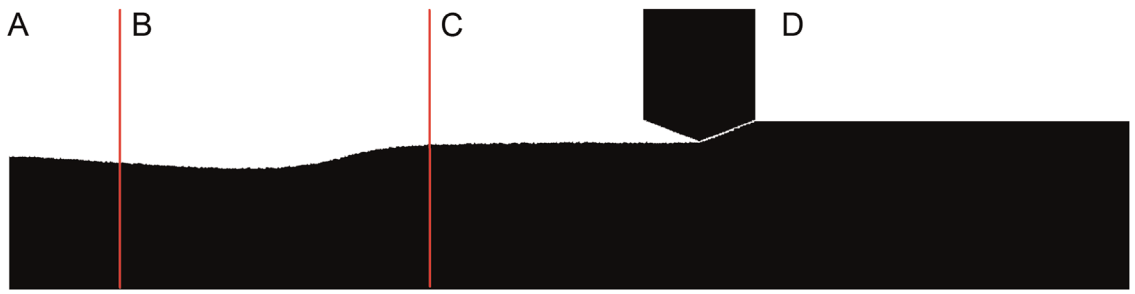

Fig. 8. Geometric characteristics of machined tool and workpiece in simulation.

The steady stage is shown in Fig. 7(g)–(h) or the region CD in Fig. 8. The shape of the electrode's end face remains unchanged after the milling is processed 1500 μm. Characteristics for this stage are as follows:

1. The electrode becomes cone-shaped and the cone angle remains steady.
2. The depth of the cavity remains unchanged, which is a little smaller than layer thickness.

Since both the horizontal and the vertical movement of the electrode can be considered as continuous, the relative movement of the electrode for the workpiece can be described as path *ab* in Fig. 9. Because of the resultant movement of the electrode, the tilting end face of the electrode is formed. With the self-spinning of the electrode, the electrode becomes conic eventually.

5. Experiment results and analysis

To verify the effectiveness of the simulation, an experiment is conducted to examine whether the cone angle of the electrode and the profile of the workpiece are in accordance with the result of the simulation in Section 4. Moreover, to verify the accuracy of the simulation, experiments with different layer thickness are conducted to compare experiment results and simulation results regarding the cone angle.

5.1. Experiment process

Experiments are carried out on CHARMILLES ROBOFORM 35 machine, with TROOP 7740Z Wire EDM machine as the cutter. The workpiece is 1Cr18Ni9Ti with thickness of 3 mm. Degree of level for workpiece is adjusted to be below 0.01 mm by TESA lever probe. The tungstic electrode with a diameter of 200 μm and a roughness of Ra0.03 after metallographic grinding is used in the experiment. The rotation speed of the electrode is kept as 200 r/min. The tool wear ratio is measured as 11.9%.

Based on the fix-length compensation method, the compensation length is calculated according to the relative parameters. With the compensation length, the machining path is programmed.

After processing, milled sections for cavity are observed on Zeiss confocal microscopy. Then the shape of the electrode is obtained indirectly by measuring the cross section of the workpiece, for it has the same pattern as the cavity.

All the experiment apparatuses and detailed machining conditions are listed in Tables 2 and 3 respectively.

5.2. Electrode shape

In order to verify the effectiveness of the simulation, an experiment with the same parameters as those in simulation in Section 4 shown in Table 1 is carried out. Here the layer thickness is 43.5 μm, the compensation length is 60 μm, the compensation accuracy is 1 μm and the machining length is 4 mm.

Table 2
List of experimental apparatus.

Item	Model
Machine	CHARMILLES ROBOFORM 35
Machine	TROOP7740Z Wire EDM machine
Post-processor	Metallographic Mosaic machine
Post-processor	Metallographic grinder
Observer	Zeiss confocal microscopy
Gauge	TESA lever probe

Table 3
Machining conditions.

Item	Unit	Value
Tool material	\	Tungsten
Workpiece material	\	1Cr18Ni9Ti stainless steel
Dielectric fluid material	\	Kerosene-based mixture
Tool diameter ($2R_t$)	μm	200
Tool polarity	\	+
Open circuit voltage	V(DC)	200
Peak gap current	A	0.5
Spark-on time	μs	1.6
Spark-off time	μs	6.4
Spindle speed	RPM	200
Tool wear ratio (θ)	\	11.9%

Fig. 10 shows the simulation results of the electrode shape and the bottom profile of the workpiece, while Fig. 11 presents the confocal microscopy of the workpiece after machining the cross section curve and longitude section curve. A comparison of the curves (Figs. 10(a) with 11(a) and Figs. 10(b) with 11(b)) suggests a good match between the experiment and simulation results under the condition of a layer thickness of 43.5 μm.

It is worth noting that the cavity depth of the workpiece after machining is smaller than its value in simulation, 34.0 μm versus 43.5 μm. Because the phenomenon of corona discharge existing in EDM is not considered, the simulation produces a sharp cone, shown as Fig. 10(a). However, in real EDM, a sharp cone cannot be maintained because of wear, and the worn cone-shaped electrode thus decreases the cavity depth of the workpiece because of the copy nature of EDM.

Though the cone-shaped electrodes in the simulation and the experiment have different depths because of the corona discharge, they have almost the same cone angle of 21°. The cone angle is used as the geometrical feature to represent the cone-shaped electrode in the following experiments.

5.3. Experimental and simulation results for various layer thickness

In order to verify the accuracy of the simulation, experiments with different layer thickness are conducted. Under the same conditions above, five different layer thickness values are set as 43.5 μm, 51.5 μm, 63 μm, 86.5 μm and 125 μm, and the corresponding compensation lengths are calculated as 60 μm, 50 μm, 40 μm, 30 μm and 20 μm respectively. Compensation accuracy is 1 μm [16], and the machining length is 4 mm.

The results of the experiments and the corresponding simulations are shown in Table 4. Here, the absolute and the relative error are defined respectively as

$$err = |\alpha_{simu} - \alpha_{exp}| relerr = \frac{|\alpha_{simu} - \alpha_{exp}|}{\alpha_{exp}} \times 100\% \quad (12)$$

where α_{simu} and α_{exp} are the cone angles of simulation and experiment respectively.

According to the comparison between experimental and simulation results, shown in Fig. 12, the two results fit well when the layer thickness is less than 85.5 μm, with a relative error of less than 4%.

When the layer thickness is larger than 85.5 μm, errors increase and the cone angles in simulations become much smaller than those in experiments. When layer thickness reaches 125 μm, the corresponding error reaches 22.76%. Such large errors are a

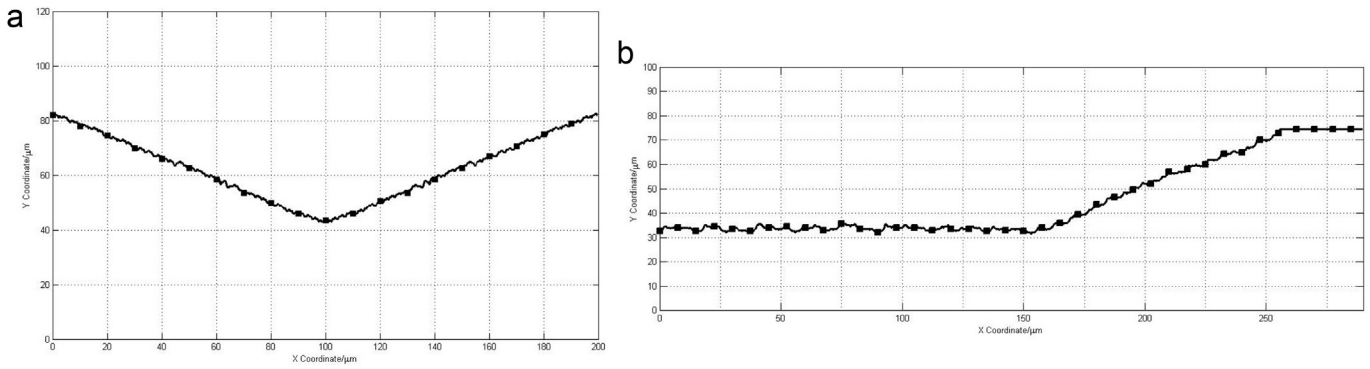

Fig. 10. Simulated results of tool and workpiece when the layer thickness is 43.5 μm: (a) tool and (b) workpiece.

result of the simplification of the model. For example, the corona discharge is excluded from modeling, and the shape and size for craters are estimated.

As Fig. 12 shows, the cone angle of the electrode in real EDM increases as the layer thickness increases, while in simulation the cone angle converges rapidly when the layer thickness exceeds 85.5 μm.

In summary, the simulation model for electrode cone angle fits well with experiments with a layer thickness of 85.5 μm and less. As the layer thickness of less than 63 μm is commonly adopted in real machining process, with a corresponding cone angle of less than 33°, such simulation model accords in most machining processing with fix-length compensation.

Table 4
Results of experiment and simulation.

Item	Unit	Values				
Layer thickness (H_{comp})	μm	43.5	51.5	63	85.5	125
Compensation length (L_{comp})	μm	60	50	40	30	20
Experimental value (α_{exp})	μm	21.08	26.1	32.1	38.9	49.2
Simulation value (α_{simu})	μm	21.06	26.67	32.16	37.38	38.01
Absolute error (*err*)	μm	0.14	0.57	0.06	1.52	11.2
Relative error (*relerr*)	\	0.6306%	1.418%	0.1869%	3.907%	22.76%

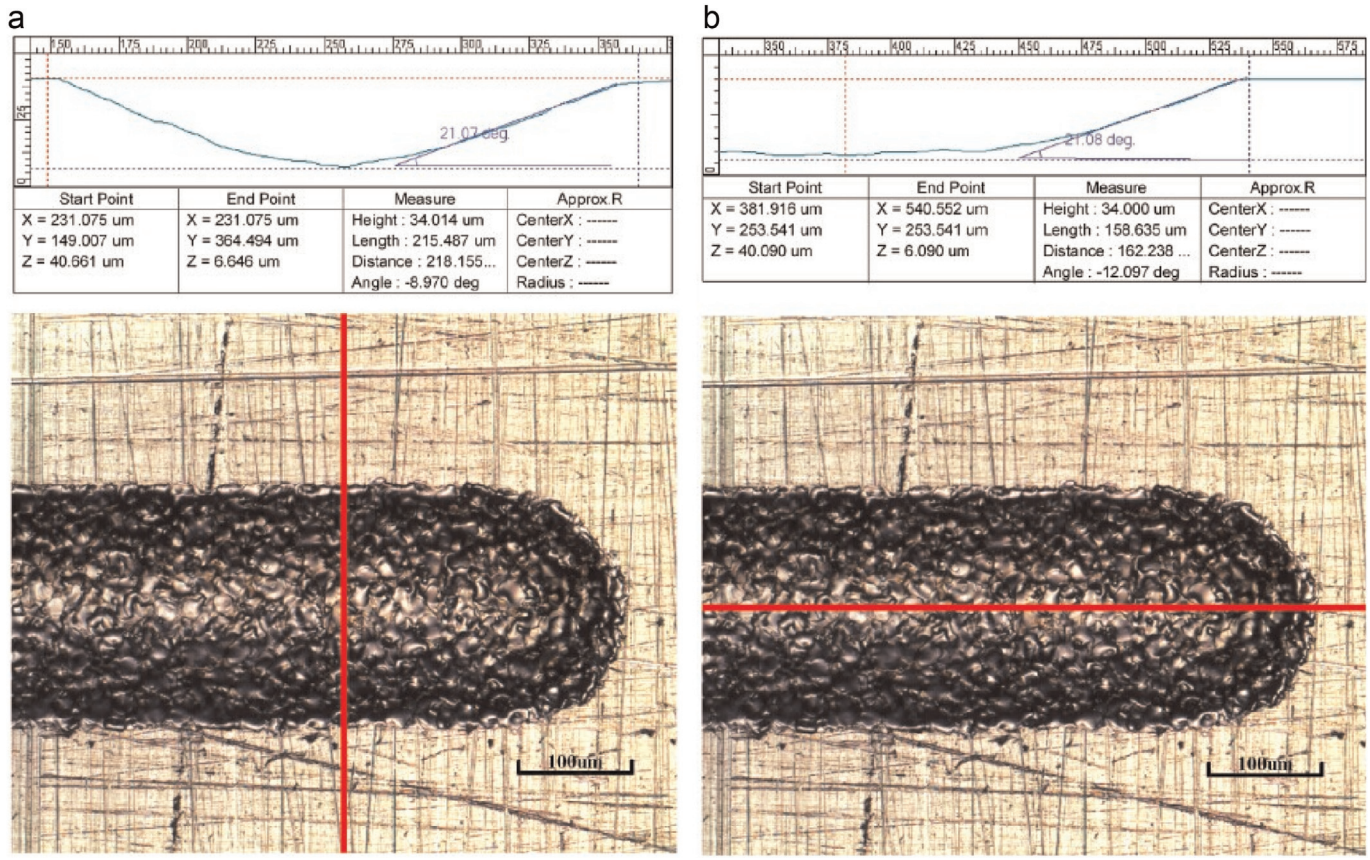

Fig. 11. Actual machined results of workpiece under the Zeiss confocal microscopy when the layer thickness is 43.5 μm: (a) cross section and (b) longitude section.

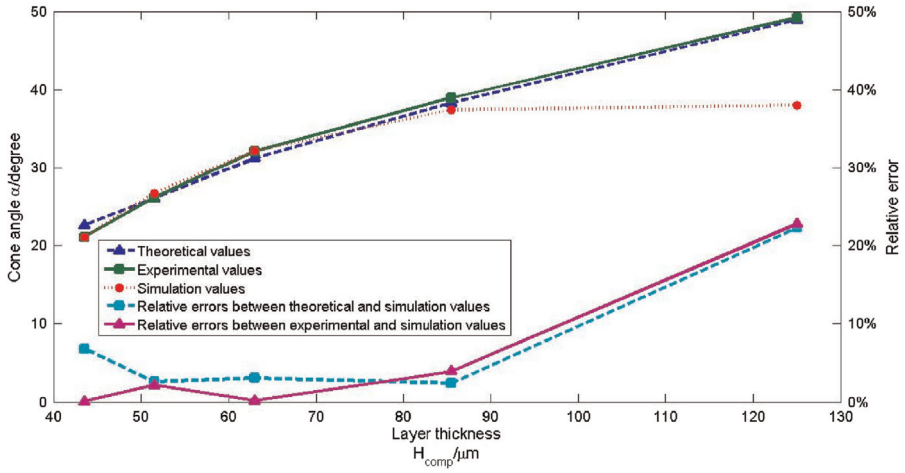

Fig. 12. Comparison between experimental and simulation results.

6. Conclusions

In this study, a two-dimensional geometrical simulation is developed for micro-EDM fix-length compensation milling with cylindrical tool.

First, the tool and the workpiece were geometrically and mathematically modeled as two-dimensional matrices. Two-dimensional absolute and relative coordinate systems are set for positioning the electrode in the machining processing.

Next, the machining process was divided into three parts including sparking, horizontal feeding and vertical feeding. Sparking focuses on searching for sparking point and the removal of the electrode and workpiece. Key points on horizontal include judgment of conditions for feed and updating positions for electrode. Priority of vertical feeding is of great importance in the third part.

Finally, a series of experiments were conducted in order to verify the effectiveness and the accuracy of the simulation.

In these ways, the cone angle is predicted precisely and explained properly.

Based on the comparison of both experiments and simulation, several conclusions can be drawn:

1. The cone angle of the electrode in fix-length compensation is caused by both the face and peripheral milling in horizontal and vertical feeding. In other words, the cone angle is formed through the relative motion of electrode along the workpiece.
2. The cone angle is a function of compensation parameters and tool wear ratio. The cone angle will monotonically increase to a limit when the layer thickness increases.
3. This simulation precisely predicts the profile of the electrode and the workpiece in the fix-length compensation process when the layer thickness is less than 85.5 μm.

As layer thickness larger than 85.5 μm is uncommon in real processing, this model can make accurate predictions for most of real processing with fix-length compensation methods. In actual processing, these accurate predictions help to optimize the compensation parameters for the next procedures to eliminate the impact of cone angle on the electrode as well as to avoid the insufficient compensation or over compensation.

Future work needs to further analyze of large errors when layer thickness grows large. Meanwhile, theories for fix-length compensation model need to be revised accordingly. Besides, corona discharge should be considered in the model, and algorithms of simulation need to be improved for higher efficiency and be extended to three-dimensional model.

Acknowledgements

The project is supported by the National Science Foundation China (Grant no. 51205252).

References

[1] Filip Staelens Snoeys, Raymond, Willem Dekeyser, Current trends in non-conventional material removal processes, CIRP Ann. Manuf. Technol. 35 (2) (1986) 467–480.
[2] K.H. Ho, S.T. Newman, State of the art electrical discharge machining (edm), Int. J. Mach. Tools Manuf. 43 (13) (2003) 1287–1300.
[3] Duc Truong Pham, et al., Micro-edm recent developments and research issues, J. Mater. Process. Technol. 149 (1) (2004) 50–57.
[4] Z.Y. Yu, T. Masuzawa, M. Fujino, Micro-edm for three-dimensional cavities-development of uniform wear method, CIRP Ann.—Manuf. Technol. 47(1) (1998) 169–172.
[5] C.L. Kuo, S.T. Chen, Y.Z. Wu, T. Yan, T. Masuzawa, Study on 3d micro edm, in: Proceedings of the Annual Assembly of Japan Society of Electrical Machining Engineers, 1997, p. 111–114.
[6] J-P. Kruth Bleys, Philip, Bert Lauwers, Sensing and compensation of tool wear in milling (edm), J. Mater. Process. Technol. 149 (1) (2004) 139–146.
[7] Pei, Jingyu et al., Arithmetic and experimental study of fix-length compensation based on conical bottom shape of electrode in micro-edm, in: ASME 2013 International Mechanical Engineering Congress and Exposition, 2013.
[8] Wataru Kowaguchi, Masanori Kunieda, Takashi Takita, Reverse simulation of die-sinking edm, CIRP Ann.—-Manuf. Technol. 48 (1) (1999) 115–118.
[9] Z.Y. Yu, J. Kozak, K.P. Rajurkar, Modelling and simulation of micro edm process, CIRP Ann.—Manuf. Technol. 52(1) (2003) 143–146.
[10] Yongshun Zhao, et al., Geometric modeling of the linear motor driven electrical discharge machining (edm) die-sinking process, Int. J. Mach. Tools Manuf. 44 (1) (2004) 1–9.
[11] Young Hun Jeong, Byung-Kwon Min, Geometry prediction of edm-drilled holes and tool electrode shapes of micro-edm process using simulation, Int. J. Mach. Tools Manuf. 47 (12) (2007) 1817–1826.
[12] Segon Heo, et al., Virtual edm simulator: three-dimensional geometric simulation of micro-edm milling processes, Int. J. Mach. Tools Manuf. 49 (12) (2009) 1029–1034.
[13] Elman C. Jameson, Electrical Discharge Machining, 2007.
[14] H.R. Rasmussen, J.A. McGeough, A macroscopic model of electrodischarge machining, Int. J. Mach. Tool Des. Res. 22 (4) (1982) 333–339.
[15] M.R. Patel, M.A. Barrrufet, D.D. DiBitonto, P.T. Eubank, Theoretical models of the electrical discharge machining process, i: a simple cathode erosion model, J. Appl. Phys. 66 (1969) 4095–4103.
[16] Bowen Zheng, Fixed-length compensation in micro edm milling with cone electrode (Master's thesis), School of Mechanical Engineering, Shanghai Jiao Tong University, 2014.